ASSESSING THE ABILITY TO DETECT INVASIVE PLANT SPECIES USING DRONE-BASED LEAF-SCALE VISIBLE AND NEAR-INFRARED IMAGING SPECTROSCOPY

Kelsey Huelsman
Advisors Howard Epstein and Xi Yang
University of Virginia

Abstract

Unmanned aerial vehicles (drones) are becoming increasingly popular for monitoring the spread of invasive plant species such as *Ailanthus altissima* (tree of heaven) and *Elaeagnus umbellata* (autumn olive). Because drones provide imagery with high spatial resolution, it is essential to understand whether intra-individual and intraspecific variability in fine resolution images will impede the ability to differentiate plant species. I collected images of forest canopies in northwestern Virginia, where *A. altissima* and *E. umbellata* are common, using a spectroscopic imager on a drone. Spectral signals were extracted from well-lit and representative pixels from individual trees and shrubs of known identities within spectroscopic images. Intraspecific and interspecific variability were calculated, and a partial least squares regression was used to predict the probability that individual trees and shrubs were *E. umbellata* or *A. altissima*. *E. umbellata* had low intraspecific variability compared to interspecific variability, while *A. altissima* had higher intraspecific variability. Intraspecific variability impacted classification certainty; mean probabilities of *A. altissima* (15-20%) classification were much lower than those of *E. umbellata* (60-100%), but classification was 98% accurate. These results demonstrate that despite variability within fine resolution spectroscopic images, accurate detection of target invasive plant species is still possible.

Introduction

Across the state of Virginia, invasive, non-native plants are radically altering natural environments by inhibiting the growth of native species upon which native wildlife and insects depend. These widespread changes in species composition also have broader impacts on soil chemistry and forest canopies, with feedbacks on dynamics of carbon, nutrients, water, and energy.

Land managers are making concerted efforts to control the spread of invasive plant species, a task that demands extensive ecosystem monitoring. Traditional approaches to ecosystem observation and monitoring are satellite-based and ground-based. Each approach, however, has caveats: satellite imagery covers large areas but cannot provide fine-scale details, while ground surveying, despite its ability to provide fine-scale details, is labor intensive, and only partially surveys broad areas. Unmanned aerial vehicles (drones) provide data on an intermediate scale, with much higher spatial resolution than satellite data and with more spatial coverage than ground surveys. As drones merge the benefits of more traditional satellite-based and ground-based monitoring, they are becoming an increasingly popular means to observe ecosystems, including invasive plant species monitoring.

Whereas drones are becoming increasingly popular as a vehicle for invasive plant species monitoring, spectroscopy has been and continues to be used for the remote sensing of plant and ecosystem observation. Spectroscopy, which includes a large number of narrower, contiguous bands, provides detailed spectral information (Chance et al., 2016; Kaufmann et al., 2008), which is influenced by differences in biophysical and biochemical characteristics of plants (Matongera et al., 2016; Wang et al., 2020; Yang et al., 2016), including: pigments

(Mahlein et al., 2010; Xiao et al., 2014), such as chlorophyll (Asner & Martin, 2008; Chance et al., 2016; Thenkabail et al., 2014), anthocyanins, and carotenoids (Blackburn, 2007); plant water and vegetation stress (Thenkabail et al., 2014); and leaf N, P, and K (Asner & Martin, 2008; Chance et al., 2016; Mutanga et al., 2004; Thenkabail et al., 2014). Thus, spectroscopic data, which serve as an indication of plant chemical and structural properties, vary within and across ecosystems (Martin & Aber, 1997; Ustin et al., 2004).

Spectra are strongly related to certain biochemical and structural plant traits (Jacquemoud et al. 2009; Kattenborn et al. 2019; Ollinger 2010). Generally, higher spectral variation is associated with species or trait variation (Palmer et al., 2002). Rocchini et al. (2004) and Palmer et al. (2002) found a significant relationship between spectral heterogeneity and species richness. Certain wavelengths, such as those associated with upper-canopy pigments, water, and [N], can be analyzed to determine species diversity. Variations in these wavelengths denote biochemical diversity and, therefore, species diversity. Intraspecific (within a species) trait variability, however, is sometimes similar to or even greater than interspecific (among species) variation (Jung et al. 2010; Messier et al. 2010; Leps et al. 2011; Auger & Shipley 2013).

Though imaging spectroscopy has been previously used to identify individual plant species (Mishra et al., 2017), particularly invasive species (Aneece & Epstein, 2017; Chance et al., 2016; Kganyago et al., 2017; Skowronek et al., 2017), using these spectroscopic sensors in concert with drones is a relatively new application for these technologies. Whereas a few drone-based studies have been successful in identifying individual plant species, this has been accomplished in large monocultures where the target plant is easily distinguished from the surrounding vegetation.

Additionally, drones provide spectroscopic imagery with much higher spatial resolution than satellites. In very fine spatial resolution, spectral variation among pixels will be greater than in coarser spatial resolution, which experience a smoothing effect of extreme values (Palmer 2000, 2002). It is expected, then, that spectral variation will be greater with decreasing spatial resolution. it is essential to understand the mechanisms that allow for the detection of target invasive plant species within these fine resolution images.

To explore the fundamental questions of whether variability caused by fine resolution spectroscopy impedes the ability to differentiate plant species, I collected images during the 2020 growing season from forest canopies in northwestern Virginia at the Blandy Experimental Farm (BEF), where invasive species are present and common. I address the following questions:

(1) Do intra-individual and intraspecific variability of target invasive plant species impede the ability to differentiate among species?
(2) Can the spectral signal from individual pixels be used to effectively detect target invasive plant species in an image?

Methods

Study Site

Blandy Experimental Farm (BEF), a biological field station owned by the University of Virginia, is located in the Shenandoah Valley in northwestern Virginia (39.06°N, 79.07°W). At 190 m elevation, BEF has a mean annual precipitation of 975 mm, a mean annual temperature of 12°C and a mean July high temperature of 31.5°C. It contains 80 ha of old fields in various stages of succession (Bowers, 1997).

Aerial spectroscopic data collection took place over three 1-ha fields at BEF, based on their abundance of invasive plant species. The fields are in early- to mid-successional stages and are approximately 20, 25, and 30 years in age (Figure 1; green, blue, and purple polygons, respectively). Each field is located on low-relief topography. The early successional field (E; green polygon in Figure 1A, Figure 1B) contains abundant invasive shrubs, including *E. umbellata* (autumn olive) and *Rhamnus davurica* (buckthorn) within a heterogeneous matrix of forbs, graminoids, shrubs, and trees (including the invasive tree of heaven, *A. altissima*). The 25-year-old early-to-mid-successional field (EM; blue polygon in Figure 1A, Figure 1C) contains abundant invasive shrubs, including *E. umbellata*, *R. davurica*, *Lonicera maackii* (bush or Amur honeysuckle) within a heterogeneous matrix of forbs, graminoids, shrubs, and trees, but with more prevalent trees and shrubs than the early successional field. The mid successional field (M; purple polygon in Figure 1A, Figure 2D) contains abundant invasive shrubs, including *R. davurica* and *L. maackii,* along with abundant *A. altissima,* and *L. japonica* and *C. orbiculatus* vines among forbs and native trees.

<u>Data collection and image post-processing</u>

Spectroscopic images were collected using a DJI Matrice 600 drone equipped with a high-precision GPS system and an imaging spectrometer (Nano-Hyperspec, Headwall

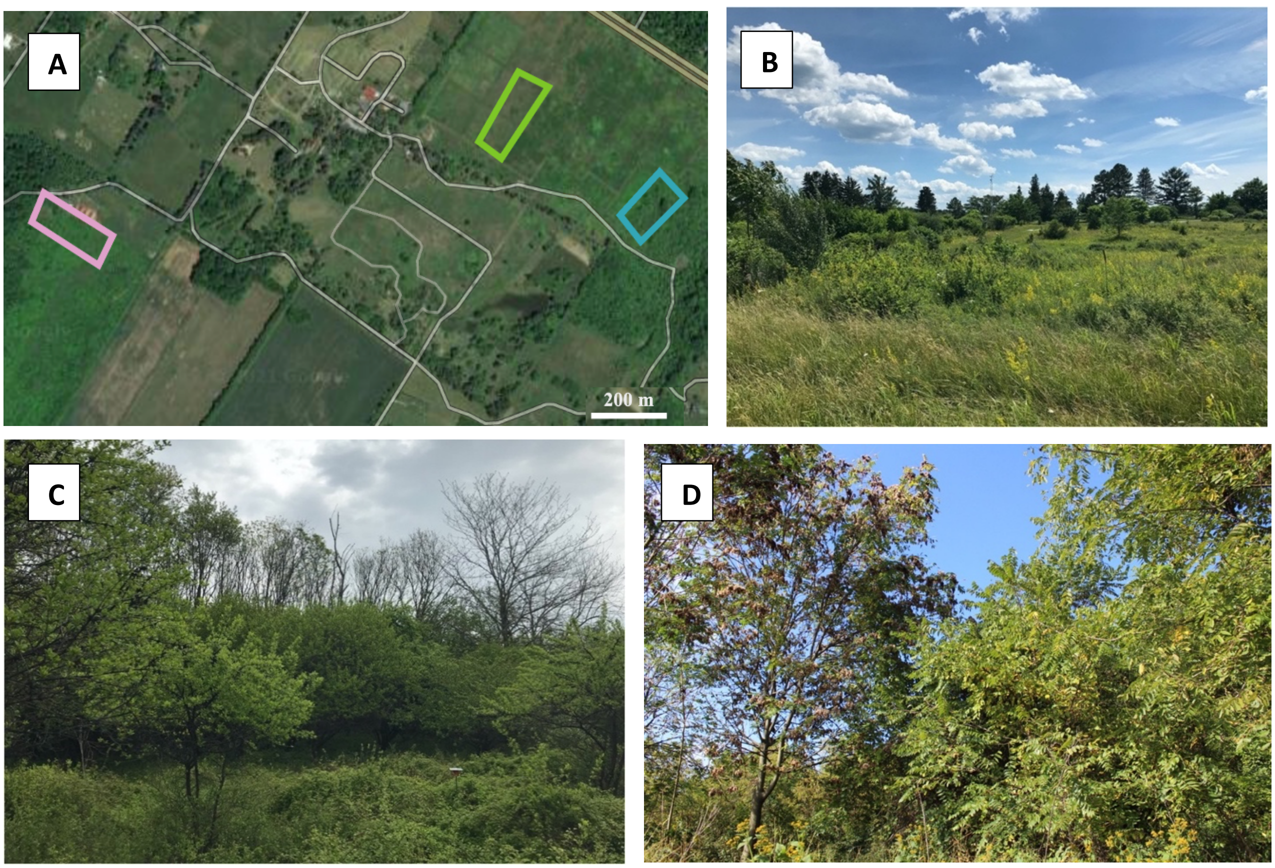

Figure 1. A. Locations of fields in which spectroscopic data were collected during the 2020 growing season. A field in early secondary succession (E), an intermediate early-to-mid successional field (EM), and a mid-successional field (M), shown in green, blue, and purple, respectively. B. Early successional field (E), which is about 20 years in age and contains abundant invasive shrubs, including *E. umbellata* (pictured on the left) and *R. davurica*. C. Early-to-mid successional field (EM), which is about 25 years in age and contains abundant invasive shrubs, including *E. umbellata*, *R. davurica* (pictured in the foreground), and *Lonicera mackii*. D. Mid-successional field (M), which is about 30 years in age and contains abundant invasive shrubs, including *R. davurica*, and *L. mackii*, along with *A. altissima* (pictured).

Photonics, Bolton, MA). The imaging spectrometer has a spectral range of 400 to 1000 nm (in the visible and NIR portions of the electromagnetic spectrum), with a spectral resolution of 2 to 3 nm over 270 spectral bands. Flight plans over each field were created using Universal Ground Control Software (UgCS), in which the drone would fly in straight lines at a consistent height of 48 m above the ground to obtain images with 3 cm pixels that could later be pieced together to form a larger image. The imaging spectrometer was programmed to capture images along the flight plan using HyperSpec III software (Headwall Photonics, Bolton, MA).

Images were collected in the middle of the growing season in late June (DOY 178), midday between 10h and 15h to reduce impacts of bidirectional reflectance distribution function (BRDF) effects and under consistent sky conditions. This date of collection was chosen for its proximity to when the National Ecological Observatory Network (NEON) collects spectroscopic images using a fixed-wing aircraft with coarser resolution (approximately 1 m resolution, compared to 0.03 m resolution). Collected spectroscopic images were adjusted for incoming and scattered solar radiation using a sampled dark reference at the time of flight and a reference tarp located in the flight scene, respectively. Using HyperSpec III software, terrain and perspective effects were removed with a digital elevation model provided by the US Geological Survey, and a mosaic of multiple images was created.

Image sampling

Individuals of 16 tree and shrub species and plant assemblages (*A. altissima*, *Celastrus orbiculatus*, *E. umbellata*, *Gleditsia triacanthos*, *Galium verum*, *Maclura pomifera*, *Juglans nigra*, *Juniperus virginiana*, *Lonicera japonica*, *Lonicera maackii, Pinus virginiana*, *Rhamnus davurica*, *rubus sp.*, *Solidago altissima*, *Symphoricarpos orbiculatus*, and graminoids) were identified in each of the three fields (E, EM, and M) using a high-precision GPS and used to catalogue individuals within imagery.

The dataset used to examine intra-individual and intraspecific variability consisted of a subset of 8 of the tree and shrub species (*A. altissima*, *R. davurica*, *E. orbiculata*, *G. triacanthos*, *M. pomifera*, *J. nigra*, *L. maackii*, and *J. virginiana*) from the three fields. If a given species was present in images of a field, up to five individuals were selected for analysis. In cases where fewer than five individuals were present, as many as were present were sampled. The dataset used to differentiate *A. altissima* and *E. umbellata* consisted of up to eight individuals of each species from each field where present.

Within the images, 15 well-lit and representative pixels were selected for spectral sampling from each individual. To remove outliers, a mean was taken across all wavelengths for each reflectance spectrum of a pixel, and a mean was calculated in a similar fashion for all 15 pixels from each individual. Any pixel within an individual that differed more than 20% from the mean of the individual was removed from the dataset. This removed approximately 10% of pixels from observation.

Intraspecific (among individuals within a species) spectral variability was quantified using a CV, using the variability among the means of each individual compared to the grand mean of the species. The CV was calculated across all wavelengths for each species. Interspecific (among species) spectral variability was also quantified using a CV, with the variability among the means of each species compared to the grand mean of all species across all wavelengths.

To examine the composition of spectral variability I used a nested analysis of variance (ANOVA) to partition the variance into different levels: inter-community (among the plant communities in fields), intraspecific (among the individuals within a species), and intraindividual (among the pixels within an individual canopy). The nested ANOVA was performed using the mean reflectance across all wavelengths from blue (450-500 nm), green (501-565 nm), yellow-orange (566-625 nm), red (626-679), red edge (680-750 nm), and near-infrared (751-950 nm) spectral regions.

To differentiate *A. altissima* and *E. umbellata*, individuals from Fields E and M were used to train an algorithm using Partial Least Squares Regression (PLS-R). To create an algorithm to detect *A. altissima*, pixels known to be *A. altissima* were recoded into 1's, representing a 100% probability that those pixels are *A. altissima*, and all other pixels were recoded into 0's, representing a 0% probability that those pixels are *A. altissima*. The same process was followed for *E. umbellata*. Once an algorithm was established, using reflectance at each wavelength to predict the probability a pixel is the species of interest for *A. altissima* and *E. umbellata*, individuals of known identities from Field EM were used to test the effectiveness of each algorithm.

Using the probability of all pixels from each individual tree, shrub, or plant assemblage, a mean was calculated, to demonstrate the overall probability that the individual was the species of interest, on a scale from 0 to 1, 0 representing 0% probability that the individual is the species of interest and 1 representing a 100% probability that the individual is the species of interest. This was done for all individuals using the algorithm to detect both *A. altissima* and *E. umbellata*.

Results

Variability

In *A. altissima*, the intraspecific spectral variability exceeds interspecific spectral variability in green, yellow-orange, and some red (around 525 to 650 nm) spectral regions and again at the red edge (around 700-720 nm). Intraspecific variability is nearly double interspecific variability around 590 nm and 610 nm (yellow-orange spectral region), and 700 nm (red edge spectral region). In *E. umbellata* intraspecific spectral variability does not exceed interspecific spectral variability in any wavelengths, though around 640 nm (red spectral region) and 700 nm (red edge spectral region), intraspecific and interspecific variability are nearly equal (Figure 2).

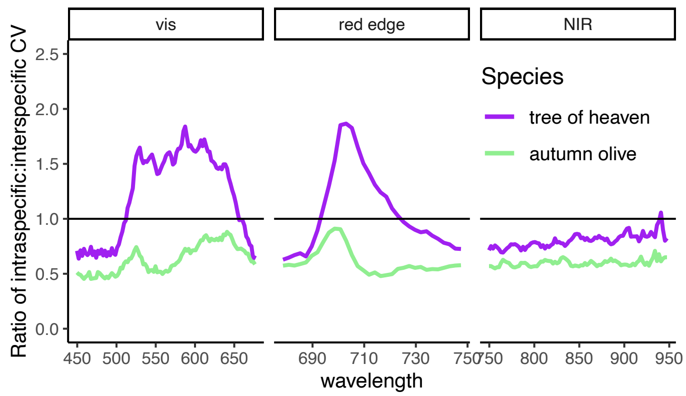

Figure 2. Ratio of intraspecific (among individuals within a single species) to interspecific (among species) coefficient of variation (CV; the variation normalized by mean) for every wavelength. Spectra are split into visible, red edge, and near-infrared regions. Ratio values over 1 indicate variability that is greater among individuals of a species than among species.

For both species, the spectral regions with greatest intra-individual variability are the green (501-565 nm) and red edge (680-750 nm). The relative contribution of intra-individual variability in the green spectral regions in autumn olive (88%) is greater than that of tree of heaven (70%). The contribution of intra-individual variability in the red edge in both species was 99%, while intraspecific variability accounted for approximately 0.8% of total variability for both species (Figure 3).

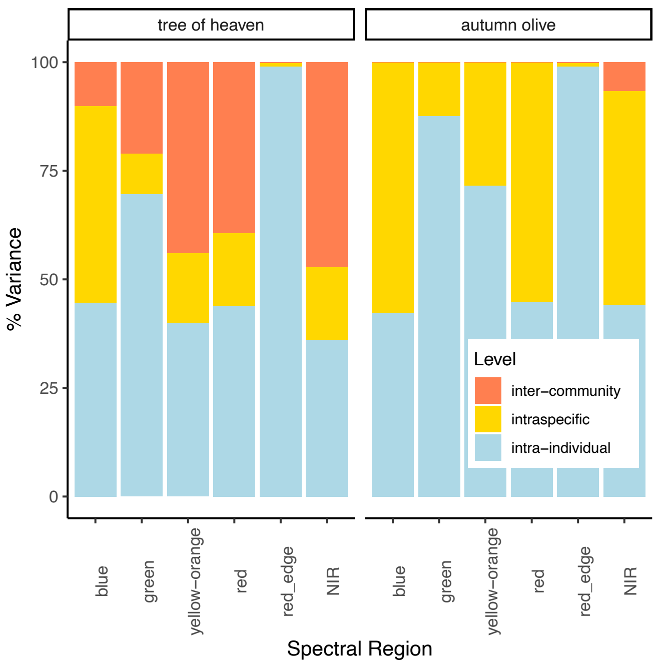

Figure 3. The results of partitioning of variance among communities ("inter-community", shown in orange), among individuals within a species ("intraspecific", shown in gold) and within individual canopies ("intra-individual", shown in light blue). The % variance is based on the relative contribution of that category to the total variance from all categories. The spectral regions are: blue (450-500 nm), green (501-565 nm), yellow-orange (566-625 nm), red (626-679), red edge (680-750 nm), and near-infrared (751-950 nm).

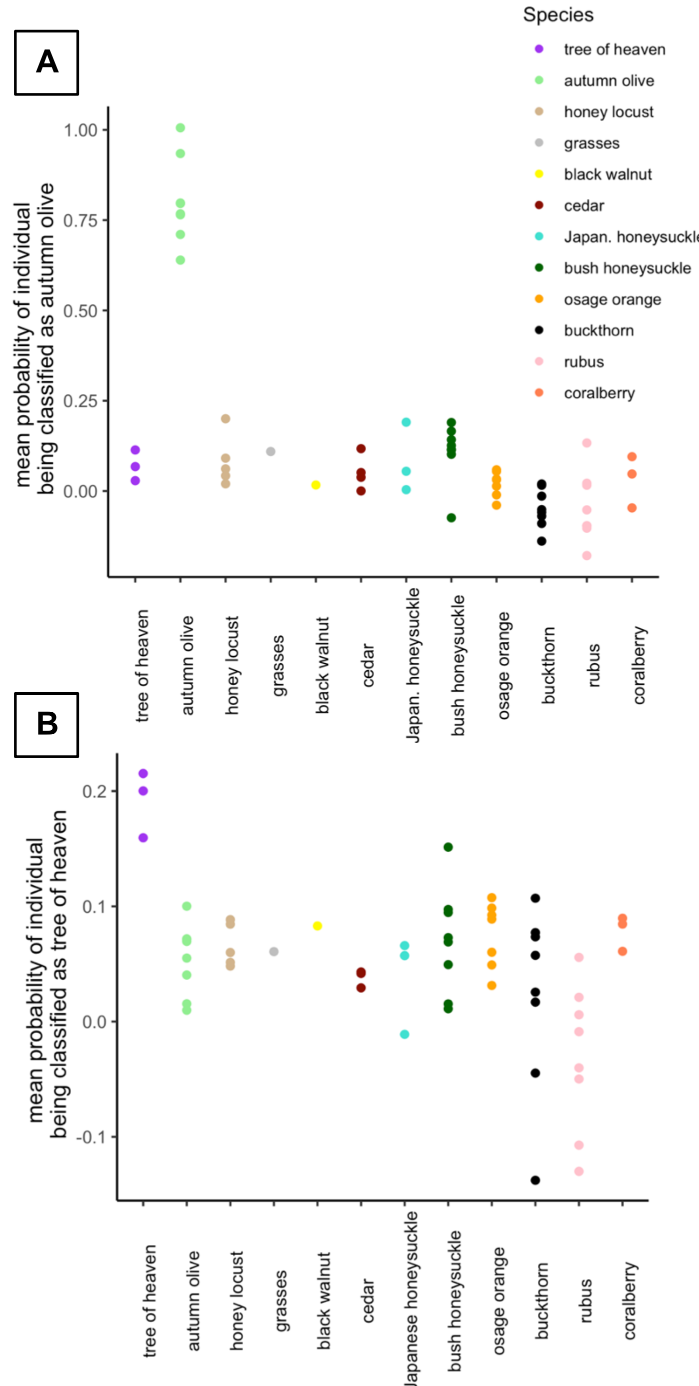

Figure 4. Accuracy of the algorithm to detect A) *E. umbellata* (autumn olive) and B) *A. altissima* (tree of heaven). Each point represents the mean probability of classification of an individual tree or shrub, taken from multiple pixels within the individual. The x-axis shows actual identities of each individual tree or shrub, which are also color-coded by species. Tree of heaven (purple) and autumn olive (light green) are the focal species.

Detection

The algorithm to detect *E. umbellata* (autumn olive) performed with much higher confidence than the algorithm to detect *A. altissima* (tree of heaven; Figure 4A). The mean probability that each *E. umbellata* individual would be classified correctly as *E. umbellata* ranged from 64% to 100% (Figure 4A). The mean probability that *A. altissima* individuals would be correctly classified as *A. altissima* ranged from 16% to 22% (Figure 5). Although the probabilities were lower for the *A. altissima* detection algorithm than for the *E. umbellata* detection algorithm, the probabilities were overall greater for individuals that were *A. altissima* than for individuals that were not. Only one individual appears to be a false positive: a *L. maackii* (bush honeysuckle) individual, which had an overall probability of 15% classification as *A. altissima* and was within range of the classification of *A. altissima* individuals (Figure 4B).

Discussion

The relatively low intraspecific variability compared to interspecific variability of *E. umbellata* likely resulted in high certainty and accuracy of classification. The high intraspecific variability of *A. altissima* compared to interspecific variability, likely resulted in much lower certainties of classification probability. Regardless, the mean probability that *A. altissima* individuals would be classified as such was still generally higher than other species, with the exception of a single individual (*L. maackii)*. This leads to the conclusion that although intraindividual and intraspecific variability can *impact* detection of invasive plant species of interest, it does not *impede* the ability to detect them.

To our knowledge, this is the first effort to identify and map invasive plant species within heterogeneous vegetation communities of the northern Blue Ridge region in Virginia. From this project our team expects to produce an effective methodology in utilizing spectroscopy to identify and locate targeted invasive plants, particularly the invasive tree *A. altissima* (tree of heaven) and shrub *E. umbellata* (autumn olive) from aerial images.

Acknowledgements

Many thanks to my advisors, Howie Epstein and Xi Yang; our collaborator from the Blue Ridge Program for Regional Invasive Species Management, Rod Walker; the Blandy Experimental Farm faculty; Lydia Mullori, who helped to sample spectra from images; Andrew Jablonski and Allie Parisien, who helped with PLS-R methods.

Literature cited

Aneece, I., & Epstein, H. (2017). Identifying invasive plant species using field spectroscopy in the VNIR region in successional systems of north-central Virginia. *International Journal of Remote Sensing*, *38*, 100–122. https://doi.org/10.1080/01431161.2016.1259682

Asner, G. P., & Martin, R. E. (2008). Spectral and chemical analysis of tropical forests: Scaling from leaf to canopy levels. *Remote Sensing of Environment*, *112*(10), 3958–3970. https://doi.org/10.1016/j.rse.2008.07.003

Blackburn, G. A. (2007). Hyperspectral remote sensing of plant pigments. *Journal of Experimental Botany*, *58*(4), 855–867. https://doi.org/10.1093/jxb/erl123

Chance, C. M., Coops, N. C., Plowright, A. A., Tooke, T. R., Christen, A., & Aven, N. (2016). Invasive Shrub Mapping in an Urban Environment from Hyperspectral and LiDAR-Derived Attributes. *Frontiers in Plant Science*, *7*. https://doi.org/10.3389/fpls.2016.01528

Kaufmann, H., Segl, K., Guanter, L., Hofer, S., Förster, K.-P., Stuffler, T., Müller, A., Richter, R., Bach, H., Hostert, P., & Chlebek, C. (2008). *Environmental Mapping and Analysis Program (EnMAP)—Recent Advances and Status*. *4*, 109–112. https://doi.org/10.1109/IGARSS.2008.4779668

Kganyago, M., Odindi, J., Adjorlolo, C., & Mhangara, P. (2017). Selecting a subset of spectral bands for mapping invasive alien plants: A case of discriminating Parthenium hysterophorus using field spectroscopy data. *International Journal of Remote Sensing*, *38*(20), 5608–5625. https://doi.org/10.1080/01431161.2017.1343510

Mahlein, A.-K., Steiner, U., Dehne, H.-W., & Oerke, E.-C. (2010). Spectral signatures of sugar beet leaves for the detection and differentiation of diseases. *Precision Agriculture*, *11*(4), 413–431. https://doi.org/10.1007/s11119-010-9180-7

Martin, M. E., & Aber, J. D. (1997). High Spectral Resolution Remote Sensing of Forest Canopy Lignin, Nitrogen, and Ecosystem Processes. *Ecological Applications*, *7*(2), 431–443. https://doi.org/10.1890/1051-0761(1997)007[0431:HSRRSO]2.0.CO;2

Matongera, T., Mutanga, O., & Lottering, R. (2016). Detection and mapping of bracken fern weeds using multispectral remotely sensed data: A review of progress and challenges. *Geocarto International*, *33*, 1–31. https://doi.org/10.1080/10106049.2016.1240719

Mishra, P., mohd asaari, mohd shahrimie, Herrero-Langreo, A., Lohumi, S., Diezma, B., & Scheunders, P. (2017). Close range hyperspectral imaging of plants: A review. *Biosystems Engineering*, *164*, 49–67. https://doi.org/10.1016/j.biosystemseng.2017.09.009

Mutanga, O., Skidmore, A. K., & Prins, H. H. T. (2004). Predicting in situ pasture quality in the Kruger national Park, South Africa, using continuum removed absorption features. *Remote Sensing of Environment*, *89*(2), 393–408. https://doi.org/10.1016/j.rse.2003.11.001

Palmer, M. W., Earls, P. G., Hoagland, B. W., White, P. S., & Wohlgemuth, T. (2002). Quantitative tools for perfecting species lists. *Environmetrics*, *13*(2), 121–137. https://doi.org/10.1002/env.516

Rocchini, D., Chiarucci, A., & Loiselle, S. (2004). Testing the spectral variation hypothesis by using satellite multispectral images. *Acta Oecologica*, *26*, 117–120. https://doi.org/10.1016/j.actao.2004.03.008

Skowronek, S., Ewald, M., Isermann, M., Van De Kerchove, R., Lenoir, J., Aerts, R., Warrie, J., Hattab, T., Honnay, O., Schmidtlein, S., Rocchini, D., Somers, B., & Feilhauer, H. (2017). Mapping an invasive bryophyte species using hyperspectral remote sensing data. *Biological Invasions*, *19*, 239–254.

Thenkabail, P. S., Gumma, M. K., Teluguntla, P., & Mohammed, I. A. (2014). Hyperspectral Remote Sensing of Vegetation and Agricultural Crops. *Photogrammetric Engineering & Remote Sensing (PE&RS)*, *80*(8), 697–723.

Ustin, S. L., Roberts, D. A., Gamon, J. A., Asner, G. P., & Green, R. O. (2004). Using Imaging Spectroscopy to Study Ecosystem Processes and Properties. *BioScience*, *54*(6), 523–534. https://doi.org/10.1641/0006-3568(2004)054[0523:UISTSE]2.0.CO;2

Wang, Z., Chlus, A., Geygan, R., Ye, Z., Zheng, T., Singh, A., Couture, J. J., Cavender-Bares, J., Kruger, E. L., & Townsend, P. A. (2020). Foliar functional traits from imaging spectroscopy across biomes in eastern North America. *New Phytologist*, *228*(2), 494–511. https://doi.org/10.1111/nph.16711

Xiao, Y., Zhao, W., Zhou, D., & Gong, H. (2014). Sensitivity Analysis of Vegetation Reflectance to Biochemical and Biophysical Variables at Leaf, Canopy, and Regional Scales. *Geoscience and Remote Sensing, IEEE Transactions On*, *52*, 4014–4024. https://doi.org/10.1109/TGRS.2013.2278838

Yang, X., Tang, J., Mustard, J. F., Wu, J., Zhao, K., Serbin, S., & Lee, J.-E. (2016). Seasonal variability of multiple leaf traits captured by leaf spectroscopy at two temperate deciduous forests. *Remote Sensing of Environment*, *179*, 1–12. https://doi.org/10.1016/j.rse.2016.03.026